FAILURE ANALYSIS AND REDESIGN OF A WAGON WHEEL SHAFT FOR SUGAR CANE TRANSPORT

ANALISIS DE FALLA Y REDISEÑO DE UN EJE DE VAGON PARA TRANSPORTE DE CAÑA DE AZUCAR

FERNANDO CASANOVA

Universidad del Valle, fesanova@univalle.edu.co

Received for review May 10 th, 2010, accepted July 9th, 2010, final version July, 14 th, 2010

ABSTRACT: In this study, a failure analysis of the wheel shafts of wagons for transporting sugar cane is carried out. Several shafts have broken with a small fatigue propagation zone and a large sudden-fracture zone. The material and load condition of the shafts were examined. Stress measurements on a vehicle with a similar suspension system were conducted to find the dynamic loads and calculate the impact factor. An impact factor higher than the one reported in the literature was found. According the manufactures, AISI 1045 steel was the material of the shaft; however, it was found that the material of some shafts did not have the specifications of AISI 1045 steel. Moreover, even if the shafts were made with good quality AISI 1045 steel, the stresses are so high that the element will fail due to fatigue. Finally, some recommendations are given to increase the reliability of the shafts, and a new design and manufacturing process are proposed

KEYWORDS: Shaft, fracture, fatigue, sugar cane transport, experimental stress analysis.

RESUMEN: En este estudio, se llevó a cabo el análisis de falla de un eje de la rueda de vagones para transporte de caña de azúcar. Varios ejes se han fracturado con una pequeña zona de propagación por fatiga y una amplia zona de fractura súbita. Se examinó el material y las condiciones de carga de los ejes. Se realizó medición de esfuerzos en un vehículo con sistema de suspensión similar para encontrar las cargas dinámicas y calcular el factor de impacto. Se encontró un factor de impacto mayor al reportado en la literatura. De acuerdo con los fabricantes, el material era acero AISI 1045; sin embargo, se encontró que el material de algunos ejes no tiene las especificaciones de este acero. Inclusive si los ejes fueran hechos con un acero AISI 1045 de buena calidad, los esfuerzos serían tan altos que el elemento fallará por fatiga. Finalmente se dan algunas recomendaciones para incrementar la confiabilidad de los ejes y se propone un nuevo diseño y proceso de manufactura.

PALABRAS CLAVE: eje, fractura, fatiga, transporte de caña de azúcar, análisis experimental de esfuerzos.

1. INTRODUCTION

In some Colombian mills, the sugar cane supply process is made using small wagons which are used to pick up the cane in the field and to deliver it to bigger wagons located on roads bordering the farm; then, the bigger wagons are used to transport the sugar cane and deliver it to the mill. In other mills, the big wagons pick up the cane directly, carry it through the field and then bring it over the road to deliver it to the mill. This methodology avoids the transfer process. But the big wagons damage and compact the soil and as the topography of the field is, in general, more irregular than the road, the working conditions for the wagon become worse.

The roughness of the field and the road impacts upon the wagon suspension systems, which can cause mechanical failures. This is the case with the shafts that connect the wheel to the wagon structure where many fractures during operation have been presented, causing time loss and increased maintenance costs. The failures are also a risk for personnel when they occur on public roads because when the shaft breaks, the wheel is decoupled.

Several fractures have occurred on shafts of 12-ton wagons where the wheel is assembled on the shaft with two tapered roller bearings and the shaft is assembled with the suspension springs by using a bolted flange. Fig. 1 shows a schematic assembly of the flange shaft. Most fractures have occurred on the change of section zone (zone A in Fig. 1) where a rounding radius of 5.5 mm exists. The flange is welded on the shaft and a few fractures on the welded zone (zone B) have also occurred. The other flange is attached to a tube that connects the wheels of the two sides and it is attached to the suspension springs. The failure analysis of some of those shafts is shown in this paper.

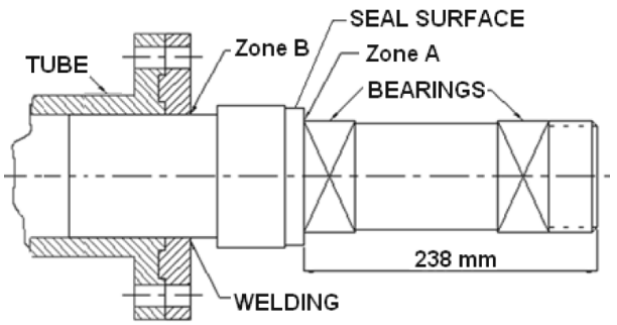

Figure 1. Schematic diagram of the shaft

2. METHODOLOGY

The failure analysis consisted of the following steps: Firstly, a visual examination of the fractured elements was performed. With the visual examination, not only the failure mechanism, but some manufacturing conditions were identified. Secondly, hardness, chemical, and metallographic analyses were done on several broken shafts to identify the kind and quality of the shaft material. Brinell hardness tests were conducted by using a Kart Frank GMBH tester under the ASTM E 10-01 standard, with a load of 1840 N, and a 2.5 mm diameter tungsten carbide ball indenter. Chemical composition analysis to two of the fractured shafts shown in Fig. 2 was carried out by using an atomic emission spectrometer. Metallographic observation was done on the change of the section zone (zone A, Fig. 1), and on the welded zone (zone B, Fig. 1), using an optical microscope and the standard method of metallographic specimen preparation. Thirdly, loads and stresses on the shaft were calculated, and the dynamic effect of road roughness was estimated by using strain measurements on the shaft of a spring suspension small vehicle. Strain was measured by using strain gauges glued between the wheel and the coupling with the suspension. Two strain gauges: one on the top, and one on the bottom of the shaft, were installed and a half Wheatstone bridge configuration was used. With this configuration, only stresses due to flexion, mainly because of vertical load, are detected. Once instrumented, the vehicle was loaded and led along an unpaved road. The tests were not performed on a sugar cane transport wagon because there is not sufficient space between the coupling with the suspension springs and the bolted flange; moreover, because part of the shaft is inside the tube, part of the load could be transferred to the tube and not detected by strain gauges. Finally, with the stresses calculated, fatigue analysis for calculating the safety factor (***n***) was made.

At the end of this paper, a new geometry and manufacturing process to assure the fatigue life of the shaft is proposed.

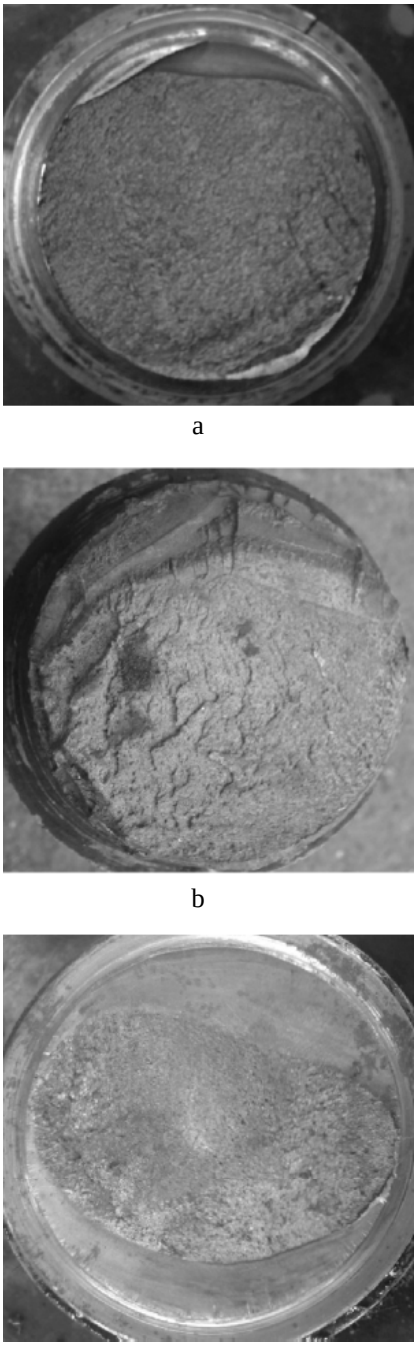

a

b

c

Figure 2. Fractured shafts

3. RESULTS

3.1 Visual inspection

Fig. 2 shows the fracture surfaces where the fatigue propagation zone and the final fracture can be clearly

appreciated. Most failures have occurred in the change of section zone (zone A) where a bearing is located; also, a few fractures have occurred on the welded zone that joins the flange with the shaft, as shown in Fig. 3a, where it can be observed that the fracture occurred from several fatigue cracks initiated on the welding. On the welded zone of the flange, cracks also have occurred, as shown in Fig. 3b. On all the fractured surfaces, it can be noted that the final fracture zone is wider than the fatigue propagation zone, indicating a high stress condition. Bad surface finish at the change of section zone was observed.

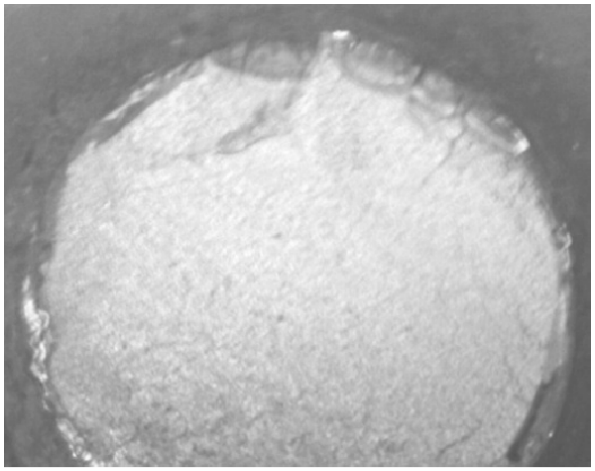

a

Figure 3. Failures at the welded zone: (a) fracture on the shaft, and (b) crack on the flange

Cracks start mainly at the bottom of the shaft because traction stresses are present in this zone due to the bending of the shaft. Because the wagons have to carry sugar cane from the field through usually irregular terrain, the shafts are subjected to fluctuating stresses and even impact when the wheels hit potholes on the road. Another event in which the loads increase considerably is when unloading the sugar cane, because it is necessary to turn the wagon over, as shown in Fig. 4. Because of the fluctuation of the loads due to impacts with road roughness, eventually the upper surface of the shaft presents traction stresses, producing fatigue propagation cracks also from the upper surface; an example of this case is shown in Fig. 2c. This change of direction of the stresses is also due to centrifugal forces during the turning of the wagon.

Figure 4. Wagon during the unloading process

3.2 Hardness and chemical composition analysis

Chemical composition of the shafts shown in Fig. 2a, and c is shown in Table 1. This table shows that the chemical composition of the material of the shaft shown in Fig. 2a, matches better with an AISI 1040 steel than with an AISI 1045 steel [1] which, according to the manufacturer, is the material that should correspond to the shafts.

Hardness was measured on the shafts shown in Fig. 2. The average values were: 203 HB, 211.4 HB, and 224.2 HB for the shafts shown in Figs. 2 a, b, and c, respectively. These results indicate no-homogeneity in the material.

Table 1. Chemical composition of the shaft shown in Fig. 2a

Shaft	C	Si	Mn	P	S	V
Fig.3a	0.42	0.26	0.76	0.03	0.025	0.03
Fig.3c	0.49	0.21	0.78	0.01	0.01	0.02

3.3 Metallographic analysis

Metallographic observation was done on specimens taken from the shafts shown in Fig. 2a, c, and Fig. 3. For the last one, the analysis was done on the welded

zone. Fig. 5 shows the microstructure of the material shown in Fig. 2a, and Fig. 6 shows the microstructure of the shaft shown in Fig 2c. Both materials present a ferritic-perlitic microstructure corresponding to annealed medium carbon steel. The main difference between the two materials is the high grain size of the material in Fig. 2a with respect to the material in Fig. 2c. This coarse grain could result in the low toughness that would explain the small fatigue propagation zone of this shaft.

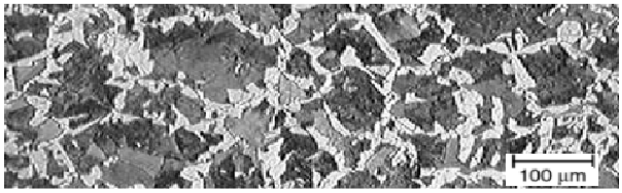

Figure 5. Microstructure of the shaft shown in Fig. 2a: ferrite (white zone) and perlite (dark zone). 100X Nital 2%

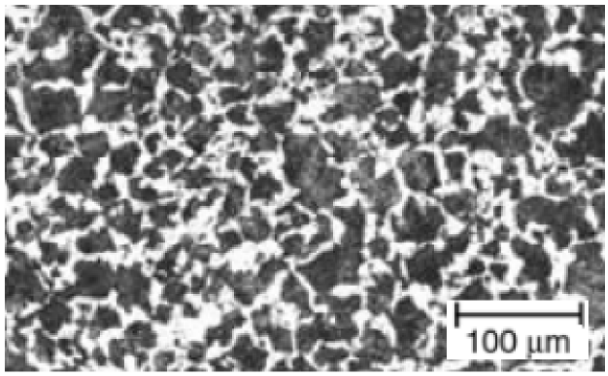

Figure 6. Microstructure of the shaft shown in Fig. 2c 100X Nital 2%

Fig. 7 shows the microstructure of the welding zone of the shaft shown in Fig. 3. The base material, the heat affected zone (HAZ), and the fusion zone are shown in Figs. 3a, b, and c, respectively. Martensite was found in the HAZ due to a lack of preheating during the welding process. This martensite is a factor that increases the risk of crack initiation in the shaft [2] and should be avoided. The fusion zone presents an acicular ferrite microstructure free of defects, where good mechanical properties are expected [2].

a

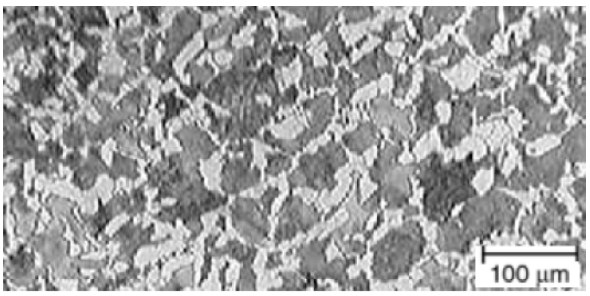

b

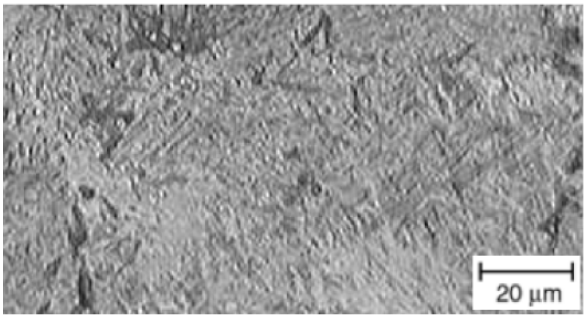

c

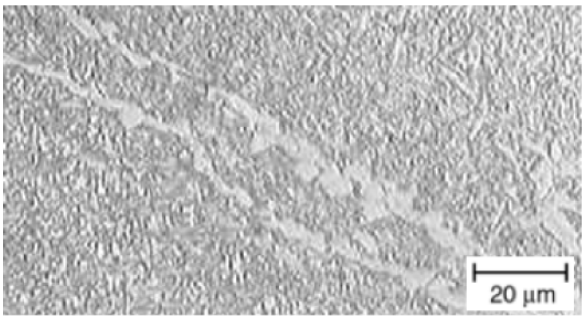

Figure 7. Shaft failed at the welded zone: (a) base material 100X, (b) HAZ 400X, and (c) fusion zone 400X. Nital 2%

3.4 Fatigue analysis

In this section, the security factor (n) at infinite life is calculated. Tensile and fatigue strength are approximately calculated from the hardness. Mean stress ($\sigma_a \sigma_a \sigma_a$) on the shafts is calculated with a static analysis assuming that the load is equally distributed among the four wheels. The maximum stress is calculated with an amplification factor that takes into account stress which rises due to the impact between the tire and the road surface.

The weight of a 12-ton capacity wagon was measured. A weight of 20.837 tons with the wagon fully loaded was obtained. On flat terrain, this load is equally distributed among the four tires; so each tire will carry 51102 N. Each wheel is assembled with two identical, single-row tapered roller bearings. The equal size and kind of the bearings allows for us to assume that the resulting force is located at the mean point between the two bearings. Tapered roller bearings also generate an axial force as Fig. 8 schematically shows. According to the bearings manufacturer, the axial force (F_a) is given by:

$$F_a = 0.47\frac{F_r}{K} \quad (1)$$

Where F_r is the radial force on each bearing (25551 N), and K = 1.45; therefore, F_a = 8282 N.

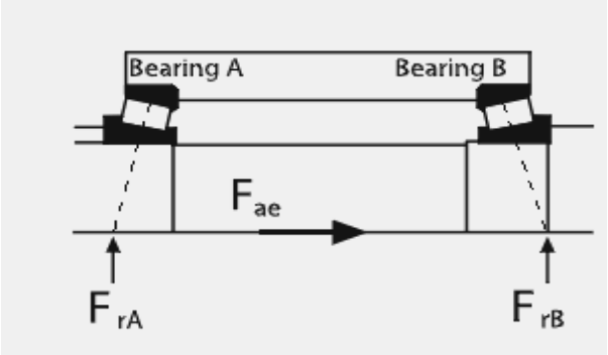

Figure 8. Forces on the shaft-bearings system

According to the bearing manufacturer, F_{rA} and F_{rB} are located at 190.5 mm and 6.35 mm, respectively, from the fracture zone. With these distances and the radial force, the bending moment and the stress produced on the failure zone can be calculated, knowing that the diameter of the shaft at the failure zone is 88.82 mm. The stress produced by the axial force produces traction stress on the failure zone, which should be added to the stress produced by the bending moment that, at the bottom of the shaft, is also traction. As this stress was calculated in static conditions, it can be taken as the mean stress. The calculated value is:

$$S_m = 74.25 MPa \quad (2)$$

The maximum stress is calculated by using the impact factor defined as [3]:

$$I = \left(\frac{R_d}{R_s} - 1\right) \quad (3)$$

Where R_d and R_s are the dynamic and static responses, respectively. Liu *et al*. [3] reported maximum impact factors of 34%; however, the roughness amplitude considered there (close to 2 cm) is not as severe as a road in bad condition where the sugar cane wagons usually have to travel. Impact factors in the same order were calculated from the results reported by Kim *et al*. [4], but the roughness studied is still low. A higher impact factor (80%) was reported by Kwasniewski *et al*. [5]. Using field tests, Moreno *et al*. [6] showed that the impact factor depends on road roughness. They found impact factors of 28.5, 50.4, and 80.5% for smooth, average, and highly rough roads, respectively.

To reduce the uncertainty of the impact factor, field tests were conducted on a small spring suspension vehicle. Fig. 9 shows the strain gauges on the vehicle shafts. 14.46 *MPa* was the stress in static conditions. Fig. 10 shows the resulting stress under dynamic conditions where the maximum value obtained was 35.11 MPa. An impact factor of 142% was found. With this impact factor, the maximum stress on the wagon shaft is:

$$\sigma_{max} = 2.42 S_m = 179.68 MPa \quad (4)$$

And the alternating stress is: $S_a = 10.43 MPa$.

The endurance limit (S'_e) of the material can be estimated by using the simplified equation [7]

$$S'_e = 0.5 S_{ut} \quad (5)$$

The ultimate tensile strength (S_{ut}) was approximately calculated with the hardness ($S_{ut} = 500 HB$); the value obtained is 727 *MPa*.

To predict the fatigue strength (S_e), the endurance limit has to be multiplied by several modifying factors, *i.e.*, surface (K_a), size (K_b), environmental (K_c), temperature (K_d), and stress concentration (K_e) [8]. S_e is given by:

$$S_e = K_a K_b K_c K_d K_e S'_e \quad (6)$$

The surface factor was obtained by using Fig. 7.7b from Ref. [7]. The roughness parameter, Ra, was measured by using a *Mitutoyo* roughness tester. The roughness obtained was Ra = 2.62 µm and the factor was approximately K_a = 0.8. The size factor is given by:

$$K_b = 0.869 d^{-0.112} \text{ [8]} \quad (7)$$

Where d is the shaft diameter (88.9 mm). The value obtained is K_b = 0.75. The environmental and temperature factors have a value of 1 in this instance. Factor K_e is giving by:

$$K_e = \frac{1}{K_f} \quad (8)$$

And K_f is the stress concentration factor given as:

$$K_f = 1 + q(K_t - 1) \quad (9)$$

Where K_t is the geometric stress concentration factor. The radius on the shaft change of section (the failure zone) is 5.55 mm (7/32 in), which is the maximum allowed by the bearing. With this value, the geometric stress concentration factor is 1.9 [8]. The notch sensitivity (q) for the AISI 1045 steel is approximately 0.8 [8]. By replacing the values, the factor obtained is K_e = 0.5, and the fatigue strength is $S_e = 109.3 MPa$.

The safety factor was calculated by using the modified Goodman approach given as:

$$\frac{S_a}{S_e}+\frac{S_m}{S_{ut}}=\frac{1}{n}\frac{S_a}{S_e}+\frac{S_m}{S_{ut}}=\frac{1}{n} \quad (10)$$

The value obtained for *n* is 0.93, meaning that the shaft will fail because of fatigue. This security factor could be even lower because impact factors higher than 142% could be present in the shaft when the wagons enter the sugar cane *field*, which is rougher than any road.

Figure 9. Strain gauge on the shaft of a spring suspension vehicle

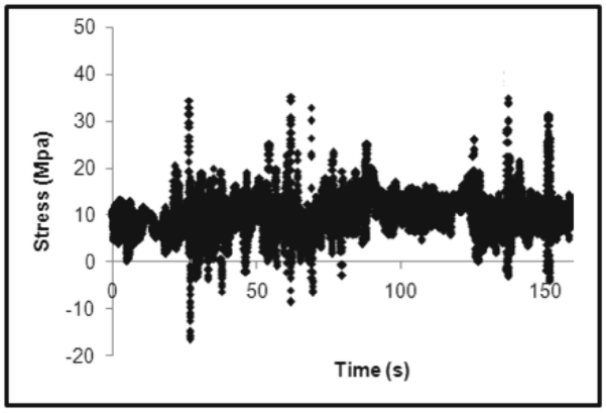

Figure 10. Stresses on the shaft

4. DISCUSSION

Visual inspection allowed us to determine the existence of fracture problems in the change-of-section zone and in the welded zone. The martensite found in the HAZ is a factor that increases the fracture risk due to its low toughness. This could be improved with appropriate preheating and post-welding heat treatment. The chemical composition showed that some shaft materials are not AISI 1045 steel, as specified by the manufacturer; also, the difference in grain size showed that the materials come from different manufacturing processes.

A first step in decreasing failures is to control the quality of materials used.

Although the impact factor found in this study was higher than that reported by other studies, even higher impact factors should be present when the wagon enters the sugar cane field or when the wagon car is turned to unload the cane. During this unloading process, impact occurs when the crane operation is not carefully performed.

The fatigue analysis showed that even if the shaft were made of good quality steel, it would be in risk of failure. Even greater risk of failure exists if a material without quality control is used.

5. REDESIGN

Several actions should be undertaken to decrease failures: First, material quality should be controlled. Second, the quality of the machining process should be improved to decrease the stress concentration, mainly at the fracture zone. Third, a forging process should be implemented rather than a welding process. Welding on the flange produces misalignment and residual stress in addition to the metallurgical problems. These factors increase the risk of failures. Fourth, changing to a stronger material like low-alloy steel should be considered. Materials with higher tensile strength and good surface finish will improve fatigue resistance. Finally, increasing the radius at the change of section should be explored; this will decrease the stress concentration factor, which is one of the most important factors in fatigue failures.

Diameters on the shaft are difficult to change because of the assembly with the wheel. The radius at the change of section and the diameter at the seal zone are restricted by the bearing and the seal. To increase the radius of the rounding at the changing of section, eliminating the section of contact with the seal is proposed. On the new radius, a ring was placed on which the bearing was supported laterally and the seal was in contact in radial direction. Fig. 11 shows a section of the new shaft. The radius was increased to 12.7 mm (½ in). With the new radius, the new K_t is 1.5 and K_e = 0.71. The decrease in the stress concentration factor increases the fatigue strength of the shaft and improves its reliability. If the safety factor is calculated again under the new conditions, the result

is $n = 1.1$, meaning that the shaft has infinite life. With the change in the shaft geometry, the increase in the bending moment is low because the distance between the resultant force and the maximum stress point is increased by only 3.175 mm (1/8 in), as seen in Fig. 11.

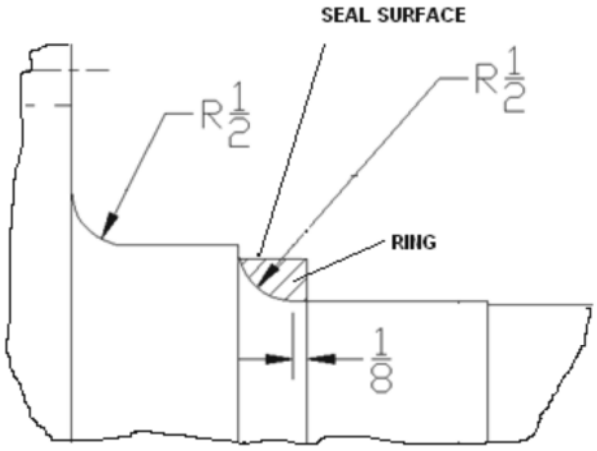

Figure 11. Section of the proposed shaft

A more adjusted design can be made by using Miner's rule to calculate an equivalent stress from the measured stress and obtaining a shaft designed for a determined period of time. More advanced methodologies than those used here can be found in the literature [9-11] and can be used to achieve a more adjusted and efficient design. Those methodologies were not used in this study because a finite life design is not adequate in this case due to the high costs of replacement of shafts and the danger of a fracture.

6. CONCLUSIONS

In several shafts, no uniform materials were found, evidencing poor material quality control. The welding process and surface finish should be improved to decrease stress concentration factors and low-toughness microstructures.

Strain measurements showed that impact factors higher than those reported in the literature are present in spring suspension vehicles moving on unpaved roads. Shafts made of the current material and with the current geometry, have a high risk of failure. A simple change in geometry by increasing the radius of rounding at the change of section zone, significantly increases the reliability of the shafts.

ACKNOWLEDGEMENTS

The author thanks the Vice-Rectory of Research at the *Universidad del Valle* for the support for this work

REFERENCES

[1] ASM HANDBOOK, Vol. 1, Properties and selection: Irons, Steels, and High Performance Alloys, 2004. p. 249.

[2] KOW, S., Welding metallurgy, Wiley & Sons, Second edition, New Jersey, 2002, p. 238.

[3] LIU, C., HUANG, D., WANG T., Analytical dynamic impact study based on correlated road roughness, Computers and Structures, 80, 1639-1650. 2002.

[4] KIM, C.W., KAWATANI, M, KIM, K.B., Three-dimensional dynamic analysis for bridge-vehicle interaction with roadway roughness, Computers and Structures, 83, 1627-1645, 2005.

[5] KWASNIEWSKI, L., LI, H., WEKEZER, J., MALACHOWSKI, J., Finite element analysis of vehicle-bridge interaction, Finite Elements in Analysis and Design, 42, 950-959, 2006.

[6] MORENO, A., TERAN, J., CARRION, F., Efecto de la rugosidad de carreteras en el daño a vehículos, Publicación técnica No. 139, Sanfandila, Qro, 2000.

[7] HAMROCK, B., JACOBSON, B., SCHMID, S., Elementos de máquinas, McGraw Hill, México, 1999. p. 268-83.

[8] SHIGLEY, J., MITCHELL, L., Diseño en ingeniería mecánica, 4ª edición, McGraw Hill, México, 1985. p. 307-313.

[9] WANNENGURG, J., HEYNS, P.S., RAATH, A.D., Application of a fatigue equivalent static load methodology for the numerical durability assessment of heavy vehicle structures, International Journal of Fatigue, 31: 1541-1549, 2009.

[10] BOESSIO, M.L., MORSCH, I.B., AWRUCH, A.M., Fatigue life estimation of commercial vehicles, Journal of Sound and Vibration, 291: 169-191, 2006.

[11] HAIBA, M., BARTON, D.C., BROOKS, P.C., LEVESLEY, M.C., Review of life assessment techniques applied to dynamically loaded automotive components, Computers and Structures, 80: 481-494, 2002.